Stochastic classical trajectory approach to relaxation phenomena. I. Vibrational relaxation of impurity molecules in solid matrices

Mary Shugard and John C. Tully

Bell Laboratories, Murray Hill, New Jersey 07974

Abraham Nitzan[a)]

Department of Chemistry, Tel Aviv University, Tel Aviv, Israel and Bell Laboratories, Murray Hill, New Jersey 07974

(Received 6 February 1978)

We present a theory of impurity vibrational relaxation in condensed media based on computer simulation of the classical equations of motion of the impurity molecule and a small number of neighboring host atoms. The host atoms are in communication with the remainder of the lattice through the presence of stochastic forces and damping terms that are constructed from knowledge of the phonon spectrum of the solid. Temperature is introduced via the fluctuation–dissipation theorem. The method is applied here to a Cl_2 impurity molecule imbedded in an argon matrix. The dependence of energy relaxation and dephasing times on interaction parameters is monitored, and comparison is made with recent spectroscopic measurements on this system.

I. INTRODUCTION

Vibrational relaxation (VR) of impurity molecules in solids and liquids has become a subject of much experimental and theoretical work in recent years.[1–27] It has been established that direct dissipation of molecular vibrational energy to the surroundings is a relatively slow process.[1–11] The small rates result from the fact that simple condensed media do not possess internal modes with high enough frequency: the characteristic period of molecular vibrations is an order of magnitude shorter than that of modes of simple solids and liquids. For modes of high vibrational frequency pure VR can be so slow that other decay channels predominate; e.g., radiative damping,[2] interimpurity energy transfer,[2b,3b,6] electronic radiationless transitions,[5,7] transfer to medium vibronic modes, transfer to other modes of the same (polyatomic) impurity molecule,[8] and transfer to rotational modes.[10] When, however, the residual energy (resulting from mismatch between the high frequency modes) which has to be released to medium modes is small, the process may be very fast—up to the picosecond time scale.[8]

In solids, the theoretical approach to the description of impurity VR is based on the general theory of multiphonon processes,[12–14] originally used for analyzing relaxation and transfer of electronic energy in and between impurity centers in lattices,[19] and later utilized in the theory of intramolecular electronic radiationless transitions.[20] This is essentially a linear response theory and it has been moderately successful in explaining and predicting general trends such as energy gap and temperature dependence of the multiphonon relaxation rates. The same type of theory has been applied to the liquid case.[21–23] There a common alternative approach exists based on the gas phase originated viewpoint of individual collisions with the surrounding molecules.[24]

In addition to population relaxation rates, phase relaxation rates have been monitored for vibrational excitations in pure liquids.[8,25,26] It should be noted that recent theoretical work on vibrational phase relaxation[21–23,27a] is essentially a one molecule theory in which the predominant mechanism for the phase damping is the stochastic nature of the interaction between each individual molecule and its immediate vicinity. Such a theory does not take into account contributions to the dephasing rate from motions of the excited molecules relative to each other,[28] and from energy transfer processes.[29] Dephasing processes have recently been observed in time resolved experiments,[30] and corresponding effects on line shapes have been discussed.

In the present work, a new approach to the theoretical study of impurity VR in condensed media is suggested and studied. This approach is based on computer simulations of the Langevin dynamics type, where classical trajectories are computed for the impurity and a few neighboring host atoms, and where the effects of the rest of the solid are introduced by stochastic forces and damping terms in the equations of motion of the host atoms. Temperature is introduced by relating the stochastic force and damping through the fluctuation dissipation theorem.

Classical trajectory computations in harmonic and anharmonic lattices is a subject of long history.[31–34] Most studies of this kind have been of the molecular dynamics type where the exact equations of motion are solved for a system of, for example, a few tens of atoms (with periodic boundary conditions) representing the monoatomic lattice. These numerical studies have

[a)]Supported in part by the Commission for Basic Research of the Israel Academy of Sciences.

 0021-9606/78/6901-0336$01.00

focused on the question of ergodicity and energy sharing between different harmonic modes due to the anharmonic coupling, and on the time scale for the energy transfer processes. Recently, Riehl and Diestler[35] have carried out a numerical molecular dynamics experiment on a one-dimensional lattice of identical diatomic molecules. Here, in addition to questions of ergodicity, one can study the energy migration from the high frequency molecular vibrations to the soft lattice phonons.

This dynamical problem is characterized by three different time scales: the shortest one corresponds to the period of the hard impurity oscillations; the intermediate one is given by the period for the low-frequency lattice modes; and the longest time scale corresponds to the energy transfer between these two types of motion. This last time scale can be orders of magnitude slower than the faster scales and for this reason numerical experiments on such systems are highly time consuming: information is sought about processes occurring on the slowest time scale while the equations of motion have to be integrated on the fastest one.

This, together with the fact that in a molecular dynamics experiment many equations of motion are involved, rules out such computations on real three-dimensional systems. Even in the one-dimensional case studied by Riehl and Diestler,[35] it was found necessary to work with a model where the molecular "hard" frequency was taken artificially small ($\sim 10\ \mathrm{cm}^{-1}$). This case does not correspond to a multiphonon relaxation process but to a resonance within the frequency spectrum of the medium.

The stochastic classical trajectory approach, while still hindered by the occurrence of the three vastly different time scales in the dynamics, provides a substantial simplification by reducing considerably the number of dynamical equations that have to be solved. This approach has recently been applied to the problem of an atom–solid surface collision[36–38] and was found to yield reliable results for accommodation coefficients and sticking probabilities. In particular, a good agreement was found between averaged classical and quantum mechanical results for the energy transfer.[38] In the present case we expect that the classical computations will offer the same advantages and also be subject to similar disadvantages as in the atom–surface system. The main problem lies in the temperature dependence at low temperatures which will not, of course, be represented correctly by the classical behavior. Other features like dependence on the impurity frequency, on impurity internal anharmonicity and on the properties of the impurity–medium interaction are expected to be represented correctly by the classical computation.

In the next section we briefly describe the method and discuss its applicability to the VR problem. In Sec. III the particular model studied here is defined, and results of energy relaxation and dephasing calculations are discussed in Sec. IV. Finally, in the last section we present an assessment of the method and outline possible future studies.

II. STOCHASTIC CLASSICAL TRAJECTORY APPROACH

The stochastic classical trajectory method is based on the assumption that an impurity molecule in a solid interacts directly with only a small number of neighboring lattice atoms. The remainder of the lattice then has only a passive role, acting as a source or sink of energy to these neighboring atoms. Following the notation of Ref. 38, we classify atoms into three groups, impurity atoms (R), a small number of primary lattice atoms (P), and the remaining huge number of secondary lattice atoms (Q). We can write the following matrix equations governing the motions of the three types of atoms:

$$\ddot{\mathbf{X}}_R(t) = \mathbf{M}_{RR}^{-1}\,\mathbf{F}_R[\mathbf{X}_R(t),\ \mathbf{X}_P(t)]\ , \tag{1}$$

$$\ddot{\mathbf{X}}_P(t) = -\mathbf{M}_{PP}^{-1/2}\boldsymbol{\Omega}_{PP}^2\mathbf{M}_{PP}^{1/2}\,\mathbf{X}_P(t) - \mathbf{M}_{PP}^{-1/2}\,\boldsymbol{\Omega}_{PQ}^2\mathbf{M}_{QQ}^{1/2}\mathbf{X}_Q(t) + \mathbf{M}_{PP}^{-1}\,\mathbf{F}_P[\mathbf{X}_R(t),\ \mathbf{X}_P(t)]\ , \tag{2}$$

$$\ddot{\mathbf{X}}_Q(t) = -\mathbf{M}_{QQ}^{-1/2}\,\boldsymbol{\Omega}_{QP}^2\mathbf{M}_{PP}^{1/2}\mathbf{X}_P(t) - \mathbf{M}_{QQ}^{-1/2}\boldsymbol{\Omega}_{QQ}^2\mathbf{M}_{QQ}^{1/2}\,\mathbf{X}_Q(t)\ , \tag{3}$$

where $\mathbf{M}_{RR}$, $\mathbf{M}_{PP}$, and $\mathbf{M}_{QQ}$ are the matrices of masses of the impurity, primary, and secondary atoms, respectively, and $\mathbf{F}_R$ and $\mathbf{F}_P$ are the (anharmonic) forces of interaction among the impurity and primary atoms. $\boldsymbol{\Omega}_{PP}^2$ is the frequency matrix describing the harmonic interactions among the primary atoms; $\boldsymbol{\Omega}_{QQ}^2$ is the corresponding secondary atom frequency matrix; $\boldsymbol{\Omega}_{PQ}^2$ describes the harmonic coupling between P and Q atoms.

Equations (1)–(3) rest on two assumptions. The first, stated above, is that the forces on the impurity atoms R do not depend explicitly on the instantaneous positions of the secondary lattice atoms. The second is that all interactions among lattice atoms are harmonic.

Following Ref. 38, we can solve Eq. (3) formally and substitute back into Eq. (2), giving

$$\ddot{\mathbf{X}}_P(t) = -\boldsymbol{\Omega}_{eff}^2\mathbf{X}_P(t) - \int_0^t \boldsymbol{\Lambda}(t-t')\,\dot{\mathbf{X}}_P(t')\,dt' + \mathbf{M}_{PP}^{-1}\,\mathbf{R}(t) + \mathbf{M}_{PP}^{-1}\,\mathbf{F}_P[\mathbf{X}_R(t),\ \mathbf{X}_P(t)], \tag{4}$$

where

$$\boldsymbol{\Omega}_{eff}^2 = \mathbf{M}_{PP}^{-1/2}[\boldsymbol{\Omega}_{PP}^2 - \boldsymbol{\Lambda}(0)]\mathbf{M}_{PP}^{1/2}\ , \tag{5}$$

$$\boldsymbol{\Lambda}(t) = \mathbf{M}_{PP}^{-1/2}\,\boldsymbol{\Omega}_{PQ}^2\cos(\boldsymbol{\Omega}_{QQ}t)\boldsymbol{\Omega}_{QQ}^{-2}\,\boldsymbol{\Omega}_{QP}^2\,\mathbf{M}_{PP}^{1/2}\ , \tag{6}$$

and

$$\mathbf{R}(t) = -\mathbf{M}_{PP}^{1/2}\,\boldsymbol{\Omega}_{PQ}^2\cos(\boldsymbol{\Omega}_{QQ}t)\mathbf{M}_{QQ}^{1/2}\mathbf{X}_Q(0) - \mathbf{M}_{PP}^{1/2}\,\boldsymbol{\Omega}_{PQ}^2\sin(\boldsymbol{\Omega}_{QQ}t)\boldsymbol{\Omega}_{QQ}^{-1}\mathbf{M}_{QQ}^{1/2}\dot{\mathbf{X}}_Q(0). \tag{7}$$

Equations (4)–(7) follow exactly from Eqs. (2) and (3), and allow us to reduce the problem to a small set of coupled equations, Eqs. (1) and (4), describing the motion of the impurity atoms and primary lattice atoms. The effects of the remaining secondary lattice atoms are included through the complicated quantities $\boldsymbol{\Omega}_{eff}^2$, $\boldsymbol{\Lambda}(t)$, and $\mathbf{R}(t)$ appearing in Eq. (4). $\boldsymbol{\Omega}_{eff}^2$ is an effective

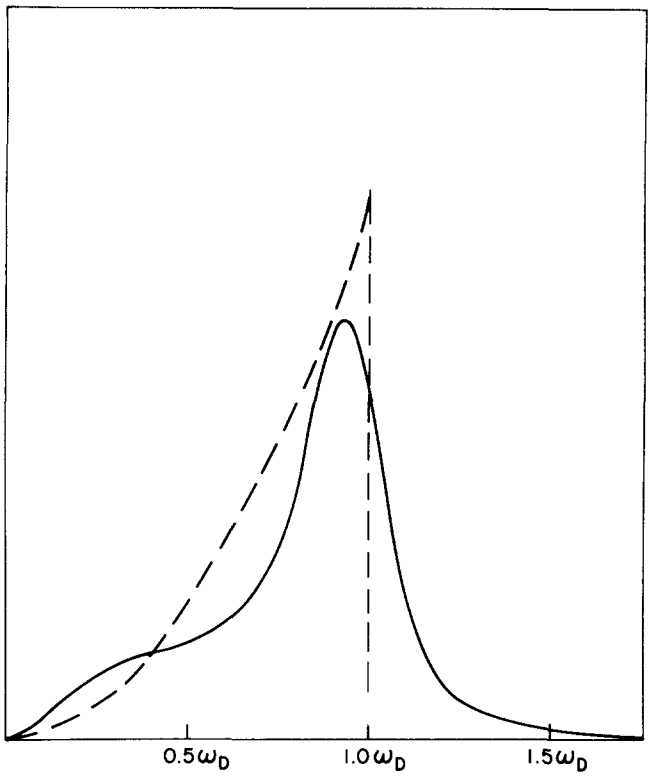

FIG. 1. Typical phonon densities of states. Solid line, from Eqs. (9) and (10). Dashed line, Debye spectrum.

frequency matrix, which is shifted from Ω^2_{PP} according to Eq. (5) due to the presence of the secondary atoms. $\Lambda(t)$ appears in Eq. (4) as the kernal of a damping or friction integral which takes account of energy flow from the localized region near the impurity to the rest of the lattice. $R(t)$ is a fluctuating force which takes account of the thermal motion of the solid and is related to $\Lambda(t)$ by the second fluctuation–dissipation theorem[36]

$$\langle R(0)R\dagger(t)\rangle = k_B T M_{PP}\Lambda(t) , \tag{8}$$

where T is temperature, k_B is Boltzmann's constant, and brackets denote (canonical) ensemble average over lattice configurations.

Equation (4) does not by itself offer any real simplification of the problem, since $\Lambda(t)$ and $R(t)$ still contain the detailed dynamics of the secondary lattice atoms. The simplification arises from two additional steps. First, it can be shown that for translationally invariant systems, $\Lambda(t)$ is related to the phonon density of states $g(\omega)$ of the lattice. Focusing on a single lattice atom, we have

$$g(\omega) = \frac{2}{\pi}\frac{\omega^2\Lambda_c(\omega)}{[\omega^2 - \Omega^2_{eff} - \omega\Lambda_s(\omega)]^2 + \omega^2\Lambda_c^2(\omega)} , \tag{9}$$

where $\Lambda_c(\omega)$ and $\Lambda_s(\omega)$ are $\pi/2$ times the cosine and sine Fourier transforms of $\Lambda(t)$.[38] Thus, if we know the phonon spectrum of the solid, we can construct an approximate form for $\Lambda(t)$ which will best reproduce $g(\omega)$ through Eq. (9). Secondly, the fluctuating force $R(t)$ can be shown to be a Gaussian random force whose autocorrelation function satisfies Eq. (8)[36]; i.e., obtaining $\Lambda(t)$ from the phonon density of states suffices to construct $R(t)$.

In this paper we construct $\Lambda(t)$ and $R(t)$ by the procedure described in Ref. 38. We approximate the damping function by the position autocorrelation function of a damped harmonic oscillator:

$$\Lambda(t) = \Lambda_0 \exp(-\tfrac{1}{2}\gamma t)\,[\cos(\omega_1 t) + \tfrac{1}{2}\gamma\omega_1^{-1}\sin(\omega_1 t)]. \tag{10}$$

We choose the three parameters Λ_0, γ, and ω_1 to best fit the experimental phonon density of states using Eq. (9). An example of a typical phonon spectrum thus obtained is compared to a Debye spectrum in Fig. 1.

With the damping kernel approximated by the form of Eq. (10), generation of the random force $R(t)$ and numerical solution of the stochastic classical equations, Eqs. (1) and (4), can be carried out by the method described in Ref. 38. The trajectory is begun with initial conditions corresponding to the initial (experimental) excitation mechanism. At 0°K, the random force vanishes, Eq. (8), and a given initial condition produces a unique trajectory. The energy remaining in the impurity can be monitored as a function of time along this trajectory. If the excitation process produces a distribution of initial configurations, than a Monte Carlo average over initial conditions must be performed. For nonzero temperatures, due to the presence of the random force, the trajectories become stochastic; a particular initial condition can evolve into a distribution of different trajectories. An ensemble average over both initial conditions and random force variations must then be carried out.

We should point out two areas of caution in applying the stochastic classical trajectory approach to vibrational relaxation in condensed phases. First, the number of lattice modes which are represented by the stochastic terms must be large enough so that an appropriate time resolution is achieved. Thus a process which occurs on a time scale of the order of $(\omega_D/N)^{-1}$ requires more than N modes within the Debye spectrum in the construction of the stochastic terms. In our approach, all modes (with density displayed in Fig. 1) are taken into account, but when using other methods[37a] care should be taken in that respect.

The second area of caution concerns the fact that the exact phonon density of states of a simple solid will be identically zero for frequencies higher than some maximum frequency, e.g., in the Debye model for frequencies above the Debye frequency ω_D. The phonon density of states corresponding to our approximate form of $\Lambda(t)$, Eq. (10), exhibits a high frequency tail, as illustrated in Fig. 1, which falls off as ω^{-6}. In fact, we have recently developed algorithms which allow the use of mode densities which fall off as ω^{-2n} for $\omega > \omega_D$, where n is any finite integer. Such algorithms will be used for VR simulation in future work. It appears, however, that some residual tail is a necessary price we pay for the simplification procedure which reduces substantially the number of effective equations of motion we have to handle. A possible unphysical consequence of this tail lies in the fact that it provides an

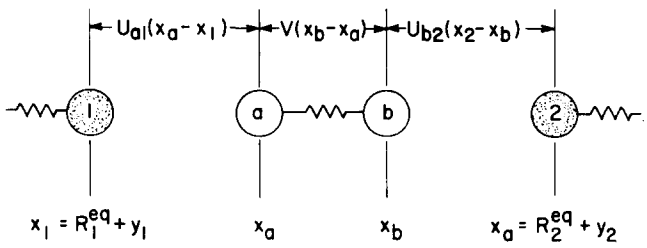

FIG. 2. Four-atom model. Atoms 1 and 2 are host atoms, atoms a and b are impurity atoms.

additional decay channel that is open even in the absence of any anharmonic coupling. This unphysical harmonic decay rate should fall off like ω^{-6} for the present model and, for large enough ω, may exceed the correct anharmonic decay rate [expected to go like $\exp(-\omega/\omega_D)$ from quantum perturbation theories]. With the parameters employed in the present computation (see next section) we estimate that zero temperature relaxation rates are not very reliable because of substantial tail interference. Fortunately, the anharmonic decay rate is a rapidly increasing function of the temperature while the harmonic one is not. Therefore the adverse effects of the tail greatly diminish at higher temperatures. More results concerning these points together with zero temperature rates calculated with more elaborate mode density functions will be published elsewhere.[39]

III. THE MODEL

Equations (1) and (3) are general in that the number of impurity atoms and the size of the neighboring lattice atom shell can be as large as we like. In this initial application of the method we restrict computations to a simplified model in which a diatomic impurity and two host atoms are treated explicitly. The model is illustrated in Fig. 2. The four atoms are constrained to move along a line. The lattice atoms are bound harmonically to fixed sites R_1^{eq} and R_2^{eq}, as shown. The impurity molecule is free to move within its lattice cage. The two impurity atoms a and b interact through a potential $V(X_b - X_a)$ which we choose to be either a harmonic or Morse potential for the present simulations. The interaction potentials U_{a1}, U_{b1}, U_{a2}, and U_{b2} are taken to be exponential repulsions.[40]

The effects of coupling to a three-dimensional lattice enter through the stochastic elements, i.e., the random forces and damping terms which are derived from a three-dimensional phonon density of states. The density of states employed is that pictured in Fig. 1, with ω_D taken to be 65 cm^{-1}, corresponding roughly to an Ar lattice. No attempt was made to accurately fit the detailed structure of the Ar density of states for this initial application. Note that the random force and damping terms acting on atoms 1 and 2 were taken to be uncorrelated. While these should strictly exhibit some correlation, this would be a very minor effect. The only correlations that should be present in these stochastic terms are those that would remain when atoms 1 and 2 are held clamped at their equilibrium positions. Thus in a collinear model (in the absence of fourth- or larger nearest neighbor interactions) the correlations are rigorously absent, and in two- or three-dimensional systems we expect them to be weak.

Because of the collinear nature of the model, rotational motion of the impurity and coupling of this rotational motion to the lattice are not included at present. In principle there would be no problem in including these effects. However, this would be likely to increase the computational time of the simulations by an order of magnitude or more. For the case of Cl_2 in Ar, the case we model below, polarization measurements have demonstrated that rotation does not play an important role.[41]

Two different experimental situations were simulated, decay following pure vibrational excitation of the impurity, and following electronic–vibrational excitation. The "standard" set of parameters used for both types of simulations are given in Table I. These parameters were chosen to model as closely as possible the Cl_2 in Ar system. However, the frequency of the impurity oscillator was taken to be 365 cm^{-1}. (The frequency of Cl_2 in its ground state is 556 cm^{-1}.) This was done in order to obtain relaxation rates which are large enough to enable us to perform relatively short (and inexpensive) calculations.

The standard set of parameters was used for all calculations reported in the next section, with at most one parameter altered to test the sensitivity of relaxation rates to that parameter. The parameters of the stochastic terms given in Table I.A were used unchanged throughout. As mentioned above, these parameters are chosen to represent a Debye lattice with Debye frequency corresponding to an Ar matrix. The parameters of the lattice atoms 1 and 2 given in Table I. B

TABLE I. Standard parameters.

A.	Stochastic parameters	
	Λ_0	0.774×10^{26} sec^{-2}
	γ	1.244×10^{13} sec^{-1}
	ω_1	0.622×10^{13} sec^{-1}
B.	Lattice atom parameters	
	Mass	40 amu
	Reg	±3.70 Å
	Ω_{eff}	0.622×10^{13} sec^{-1}
C.	Lattice–impurity interaction parameters	
	A	8.0×10^5 eV
	α	5.44 $Å^{-1}$
D.	Impurity parameters (pure vibrational excitation)	
	Mass	35.5 amu
	K	1.40×10^5 erg-cm^{-2}
	X_0	1.988 Å
E.	Impurity parameters (electronic–vibrational excitation)	
	Mass	35.5 amu
	De	0.4125 eV
	β	2.397 $Å^{-1}$
	X_0	2.228 Å

also represent Ar, with the equilibrium positions ±3.7 Å corresponding to one Ar van der Waals diameter. Thus the impurity molecule replaces a single Ar atom in the lattice. The Ar–Cl interaction parameters α and A given in Table I. C,

$$U(x) = A \exp(-\alpha x), \tag{11}$$

were chosen to fit the repulsive wall of the Ar–Ar Lennard–Jones potential.[40] Thus we have made the very crude approximation that the Ar–Cl repulsion is similar to that of Ar–Ar. For the studies of relaxation following pure vibrational excitation we employed the harmonic Cl–Cl interaction given in Table I. D. The parameters of the Morse potential,

$$V(x) = D_e\{1 - \exp[-\beta(x - x_0)]\}^2 , \tag{12}$$

employed for the electronic–vibrational excitation simulations, given in Table I. E, were chosen to best fit the $Cl_2(B\,^3\Pi)$ state potential curve.[41]

For all studies reported here, we performed an additional reference calculation in which the exponential coupling between lattice and impurity atoms was removed and replaced by a harmonic interaction. The harmonic constants were obtained by expanding the lattice–impurity interaction about the equilibrium configuration. These harmonic reference calculations were performed to demonstrate that the unphysical relaxation occurring due to the previously described high frequency tail of the phonon density of state was of negligible importance. In all cases, relaxation times for the harmonic reference calculations were at least an order of magnitude slower than for the corresponding anharmonic calculation. It should be kept in mind, however, that some contribution of the unphysical tail may persist due to mixed coupling effects. The presence of the tail is therefore expected to cause an overestimate of the relaxation rates.

IV. RESULTS OF COMPUTER SIMULATIONS

A. Pure vibrational excitation

As mentioned in the previous section, simulations of relaxation following pure vibrational excitation were performed with the standard parameters of Table I. A–I. D. The intra-impurity interaction was taken to be harmonic, so the only anharmonic interactions were the lattice–impurity exponential repulsions. Except for zero temperature runs for which only a single trajectory is required, energy relaxation and dephasing times were obtained by averaging over 10 trajectories of 100 psec (or 10^5 integration steps) each. Initial conditions for these trajectories were selected by the following Monte Carlo procedure: The anharmonic coupling was temporarily linearized and the normal modes of the resulting four atom chain were solved for. These consist of three low frequency latticelike modes, and one high frequency impurity mode. The small frequency shift between the isolated and interacting impurity molecule produced by our standard parameters is consistent with experimental observations. Initial values of the normal coordinates and momenta of the three latticelike modes were assigned by sampling at random from a Boltzmann distribution characteristic of the lattice temperature. The initial coordinate and momentum of the impurity normal mode was obtained by adding an excitation energy of 0.735 eV (~14 vibrational quanta) to the randomly chosen thermal energy in this mode. Transformation from normal coordinates back to real coordinates then supplied the initial positions and momenta of the four particles.

Energy relaxation was monitored by following the decay of the total energy of the four particle system. This procedure is equivalent to monitoring the energy of the impurity, and removes the necessity of making an arbitrary distinction between parts of an interacting system of particles. In addition to monitoring energy decay, we computed the autocorrelation function of the distance between the two impurity atoms, $\langle[X_b(0) - X_a(0)][X_b(t) - X_a(t)]\rangle$. This is a damped oscillatory function, the damping corresponding to the loss of phase coherence of the ensemble of oscillators. It is the decay time of this correlation function that we refer to as the dephasing time.

Figure 3(a) shows plots of local energy versus time for two typical trajectories. Figure 3(b) shows the same quantity averaged over 10 trajectories. We call attention to two interesting features of these plots. First, we see that in a single trajectory energy is lost predominantly in small chunks occurring at random times. This chunky behavior is smoothed out when averaged over many trajectories. This behavior is apparently due to a positive feedback mechanism in which a small leakage of energy from the impurity to nearby lattice atoms causes local heating which tends to increase the rate of leakage. This nonlinear effect appears to be very important and stands in contrast to the philosophy of linear response theory descriptions of vibrational relaxation.[13,14] It may also be in conflict with the binary collision viewpoint[24] which, although predicting energy decay in chunks, invokes chunks of much shorter duration and physically different origin (a single favorable collision vs feedback via local heating).

A second interesting feature of these trajectories is the existence of an initial transient period of very fast decay (amounting to $\lesssim$4% of the total) followed by a second (major) slower decay mechanism. Obviously, it is the second slower decay that is related to experimentally measured VR processes, and it is this slower time that will be referred to in all of the following discussions. It should be pointed out, however, that first, there is no reason to believe that this fast decay is an artifact of the computation, and secondly, that the time scale for the fast decay (1 psec) is achievable with present picosecond techniques. The occurrence of the fast relaxation component is probably due to dissipation of energy injected into nonlocal lattice modes during the (computer generated) excitation process. This initial local accumulation of energy in nonlocal lattice modes may further enhance the relaxation of the impurity oscillator itself because it has the effect of a higher local lattice temperature. It should be pointed out that this effect may in principle occur also under

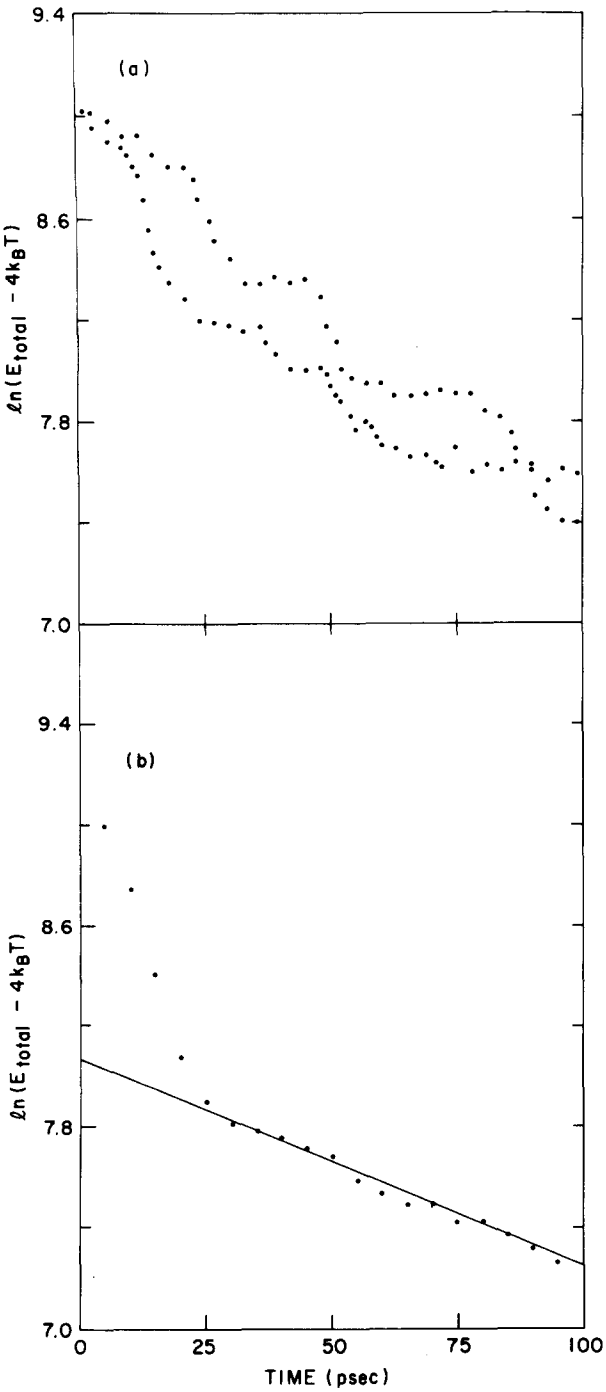

FIG. 3. (a) Local energy vs time for two typical trajectories. Standard parameters (Tables I.A–I.D) are used, except $K = 0.93 \times 10^5$ erg-cm^{-2}. (b) Average over 10 trajectories.

real-life excitation conditions. Of course, when the excitation takes place into the phonon sideband a fast initial dissipation is expected. However, also when the excitation takes place into the zero phonon line some nonlocal modes are excited which couple to the high frequency local modes by the anharmonic part of the impurity lattice interaction potential. It is interesting to note that a fast decay component was actually observed in the fluorescence monitored $1 \rightarrow 0$ vibrational relaxation of the $B^2\Sigma^+$ state of C_2^- imbedded in solid rare gas matrices.[7]

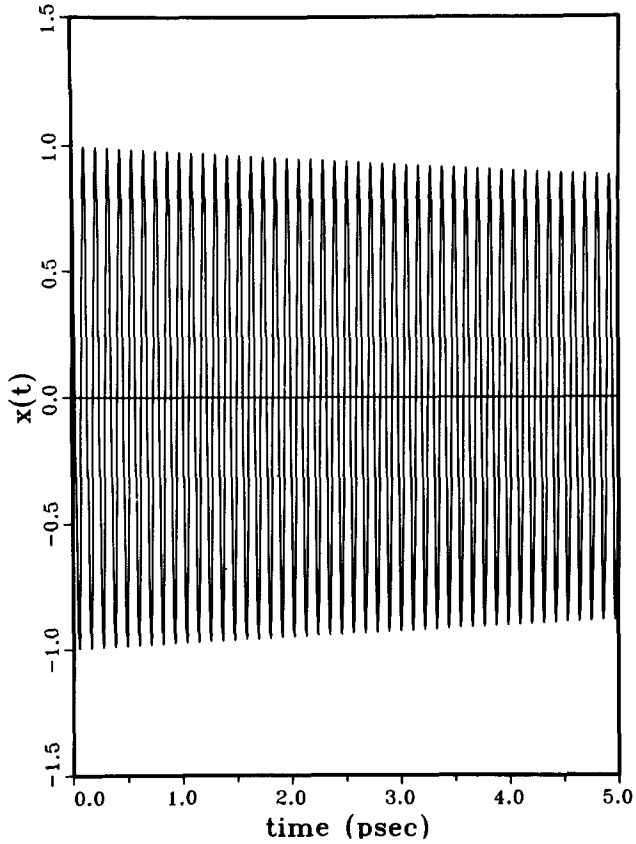

FIG. 4. Autocorrelation function of impurity internuclear separation. Standard parameters (Tables I.A–I.D) are used, except impurity force constant $K = 0.93 \times 10^5$ erg-cm^{-2}.

Figure 4, a typical autocorrelation function of impurity internuclear separation, illustrates the slowness of decay relative to the impurity oscillation frequency. Figure 5 shows the envelope of the autocorrelation function of Fig. 4, plotted on a semilog scale so that the inverse of the slope equals the decay time; i.e., the dephasing time. Figure 6 is a similar plot of the envelope of the autocorrelation function for simulation of relaxation following electronic–vibrational excitation, to be discussed below. Dephasing times are somewhat faster

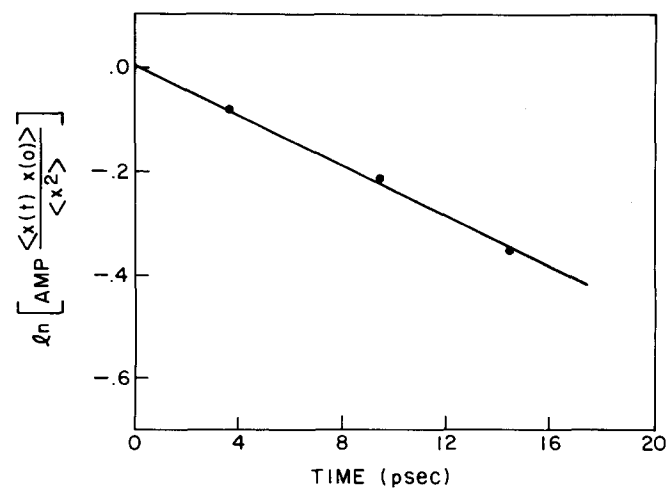

FIG. 5. Envelope of autocorrelation function of Fig. 4.

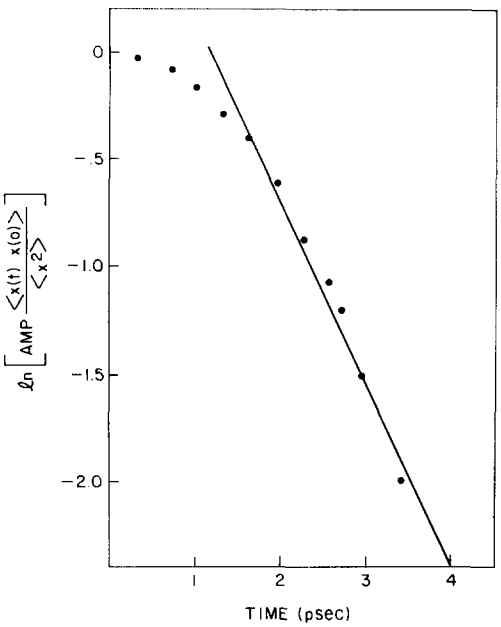

FIG. 6. Envelope of autocorrelation function of impurity internuclear separation for Morse oscillator with standard parameters, Tables I.A–I.C and I.E, and $v' = 13$.

than energy relaxation times in almost all cases.[42] In addition, at very small times dephasing follows Gaussian decay, going over to exponential (Lorentzian) after 1 or 2 psec. This is consistent with the following physical picture. At the instant of excitation each oscillator in the ensemble is in a slightly different environment (slightly different positions of neighboring host atoms), and begins to oscillate with slightly different frequency. This produces the initial Gaussian loss of coherence. Soon, however (on the time scale of lattice atom motion), the initial frequency of each oscillator is forgotten and dephasing occurs due to frequency fluctuations arising from the stochastic motion of the lattice. This produces the observed exponential decay.

1. Dependence on A

We have examined the dependence of the major (slow) energy relaxation rate and of the dephasing time (which we monitor only after the onset of the slow energy decay) on several of the parameters of our model. We discuss first the dependence on the strength of the exponential impurity–host repulsion, A of Eq. (12). Results are shown in Table II for all parameters given by their standard values of Table I, except for A, which is varied. The temperature of these runs is 50 °K. Both energy relaxation and dephasing rates increase markedly with increasing A. The variation of the energy relaxation rate with A is somewhat more rapid than the perturbation theory expectation[13,14] of proportionality to the square of the anharmonic interaction strength $A^2 \exp(-2\alpha\Delta X)$, while the variation of the dephasing rate follows this expression quite closely. Note that this expression involves ΔX, the equilibrium separation of the impurity and near-neighbor lattice atom, which changes somewhat when A is altered. Thus we would not expect, and do not find, proportionality of the rates simply to A^2.

TABLE II. A dependence.

A (eV)	Energy relax. (10^{-12} sec)	Dephasing (10^{-12} sec)
4.0×10^5	2263	205
8.0×10^5	950	147
16.0×10^5	317	75

TABLE III. α Dependence.

α (Å^{-1})	Energy relax. (10^{-12} sec)	Dephasing (10^{-12} sec)
2.84	54	26
3.78	404	55
5.44	950	147
7.56	>7500	300

2. Dependence on α

The dependence of relaxation and dephasing times on the range of the interaction, α of Eq. (12), is shown in Table III. Again, all parameters are "standard" from Table I, except α. Note that the root mean square deviation of the impurity oscillator, with our standard parameters, is $\sim 7.5\times10^{-2}$ Å. In these units the standard value of the range parameter α is 0.4. Thus we are in a "weak coupling" case, $\alpha < 1$.

The energy relaxation and dephasing rates both decrease with increasing α. This is in agreement with perturbation theory predictions,[13,14] and is simply due to the fact that the anharmonic interaction $A\exp(-\alpha x)$ becomes weaker as α is increased. Notice that the collisional theories[21] of relaxation and dephasing do not contain the term $\exp(-\alpha\Delta X)$ and naive application of such theories to the impurity–lattice system may lead to the incorrect conclusion that the rates should increase with α.

3. Dependence on impurity force constant

The dependence of the energy relaxation and dephasing times on the impurity force constant K is shown in Table IV.[42] As we see, the energy relaxation rate decreases very rapidly with increasing impurity force constant while the dephasing rate varies relatively little. Both observations correspond well to experi-

TABLE IV. K dependence.

K 10^5 erg-cm^{-2}	Energy relax. (10^{-12} sec)	Dephasing (10^{-12} sec)
0.62	23	33
0.93	110	40
1.24	430	144
1.40	950	147
1.68	5015	152
2.02	>10000	156

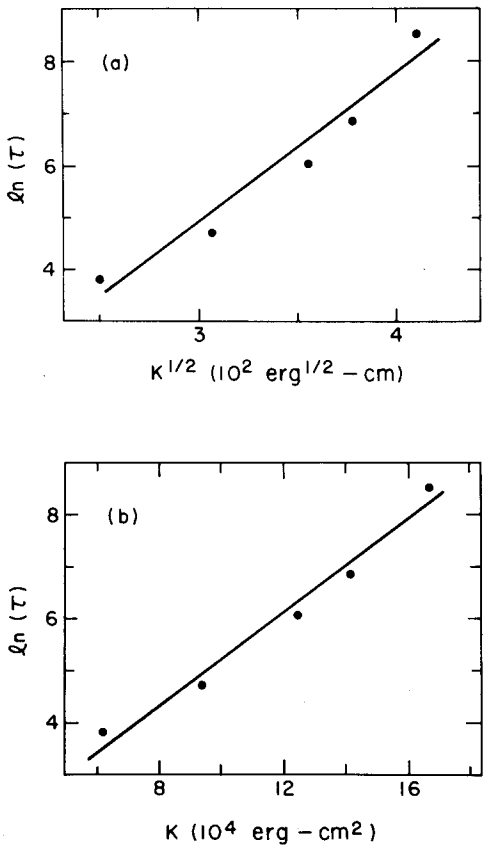

FIG. 7. (a) Plot of the natural logarithm of the energy relaxation rate vs $K^{1/2}$. (b) Plot of the natural logarithm of the energy relaxation rate vs K.

mental trends. Measured energy relaxation rates vary widly over a range of 10^{1}–10^{-12} sec, with variations of impurity force constant apparently responsible for most of this effect. Dephasing seems to be much less sensitive. A notable example is VR in pure liquid nitrogen where energy relaxation occurs on the time scale of tens of seconds[4] while dephasing occurs in picoseconds.[26]

Perturbation theory[13,14] predicts that in the "weak" and "strong" coupling limits the log of the energy relaxation rate should be proportional to $K^{1/2}$ or K, respectively. Figures 7(a) and 7(b) show that, within numerical accuracy, our results fit either relationship equally well; the present set of computations cannot distinguish between these limits.

TABLE V. Temperature dependence.

T (°K)	Energy relax. (10^{-12} sec)	Dephasing (10^{-12} sec)
25	5522	297
50	950	147
100	190	34
150	60	19
200	40	16
500	4	8

TABLE VI. Electronic–vibrational excitation.

Vibrational level V'	Energy[a] relax. (10^{-12} sec)	Dephasing (10^{-12} sec)	Exptl (Ref. 41) (10^{-12} sec)
5	2800	12	
7	960	6	
9	440	2.8	
10	290	2.6	1.1
11	340	2.4	0.9
12			0.4
13	74	1.2	0.4
14			0.3
15	63	1.1	

[a]In order to compare with decay times extracted from experimental linewidths, Ref. 41, the classical mechanical energy relaxation times appearing in this column have been multiplied by $\Delta E_v/E_v$, where E_v is the energy of vibrational level v and ΔE_v is the energy difference between the v and $v-1$ Morse levels.

4. Dependence on temperature

It can be seen from Table V that both the dephasing and energy relaxation rates are rapidly increasing functions of the temperature,[42] in agreement with both existing theoretical[13,14] and experimental[9] work. Since our approach is based on classical mechanics, however, we do not expect the temperature dependences to be relevant at very low temperatures. In particular, energy relaxation rates are seen experimentally to be independent of temperature as $T \to 0$. This behavior is also exhibited by quantum mechanical perturbation theories. By contrast, our method shows a substantial (unphysical) increase in energy relaxation rate as temperature is increased from 0 °K to 4 °K. This results from the fact that the population of a classical oscillator increases more rapidly with temperature than that of a quantum oscillator of the same frequency at low temperatures. This is particularly important for the high frequency lattice modes which dominate both the energy relaxation and dephasing processes. We therefore expect classical mechanics to overestimate the temperature dependence of the rates at low temperatures.

B. Electronic–vibrational relaxation

Bondybey and Fletcher[4] have recently reported measurements of the excitation spectrum of the transition $Cl_2(X^1\Sigma^+,\ v=0) \to Cl_2(B^3\Pi,\ v')$ in argon matrix at 4 °K. They observed that the linewidths increase significantly with increasing final state vibrational level over the range $v' = 10$–15.

We have simulated energy relaxation and dephasing in the excited $B^3\Pi$ state of Cl_2 using the parameters of Tables I.A–I.C, and the Morse potential parameters of Table I.E. The initial conditions were prescribed in the following way. A normal mode decomposition of the four-atom system was performed as before, and initial coordinates and momenta of the three lattice-type modes were selected at random from a thermal

distribution, just as in the previous simulations except now for $T = 4\,°K$. Excitation of the impurity mode was achieved using the classical Franck–Condon principle: the position and momentum of the impurity oscillator were taken to be equal before and after excitation. For each particular transition $Cl_2(X^1\Sigma^+,\ v=0) \rightarrow (B^3\Pi,\ v')$, there is a single unique value of position and momentum that satisfies this requirement. Relaxation rates were then obtained by integrating 10 trajectories of 100 psec duration (2×10^5 integration steps each).

Results are shown in Table VI. Included in this table are the experimental lifetimes estimated from the zero-phonon linewidths reported by Bondybey and Fletcher.[41] The dephasing as defined operationally in our calculations should provide a major contribution to this zero phonon linewidth. Thus the calculated dephasing times should be greater than or about equal to the experimental lifetimes, as they are. In fact, the computed dephasing times are of the correct order of magnitude and vary in the correct way with final vibrational level v'. The large difference between computed energy relaxation and dephasing times, Table VI, may indicate that energy relaxation provides only a minor contribution to the observed linewidths.

Unfortunately, we cannot expect our classical mechanical theory to be reliable for temperatures as low as 4 °K. The calculations predict a rapid increase in linewidth with increasing temperature in this range, in contrast to the experimental observation of essentially no change in linewidth from 4 °K to 15 °K.[41] Thus the qualitative agreement may be fortuitous. Even the observation that dephasing and not energy relaxation dominates the linewidth must be considered suspect.

Before leaving this example, we present one more result which we do not understand. In addition to carrying out the simulations described above using a Morse potential for the impurity, we repeated the calculations with a harmonic impurity oscillator. However, we allowed the frequency of the oscillator to vary with vibrational level v' so as to reproduce the splitting between the Morse quantum levels v' and $v'-1$; i.e., the harmonic frequency was decreased with increasing vibrational level v'. These calculations produced energy relaxation times that were very much shorter than the Morse times, and in fact agreed quite well in magnitude and v' dependence with the experimental lifetimes.[41]

V. CONCLUSIONS

We have demonstrated that numerical simulations based on classical stochastic trajectories provide a useful method for studying impurity VR processes in condensed media. The method has some obvious deficiencies: first, it is based on classical mechanics and as such will lead to incorrect results whenever quantum effects become important. Secondly, because of the high computational demands, it is limited to relatively fast processes; i.e., those occurring on time scales faster than 100 nsec. Finally, for the sake of computational convenience a model density of modes with a nonphysical high frequency tail has been employed.

As was mentioned before, we are now able to use a more physical mode density and, with computation cost being the only limitation, can approach arbitrarily close to a Debye spectrum for the stochastic terms representing the medium. For a high frequency impurity we expect that existence of the cutoff rather than the particular structure of the medium spectral density is the most important factor.

We expect that the classical nature of the method leads to unphysical results only for the temperature dependence of the relaxation rates near $T \rightarrow 0$. Other important features of the VR process, like the dependence on the impurity frequency and on the detailed impurity medium interaction, are expected to be represented well by the classical results. In this context it is important to note that the quantum nature of the impurity levels which restrict energy transfer to be in multiples of $\hbar\omega$ is represented well also by the classical equations of motion. Also, no inherent quantum effects like tunneling are expected to play an important role in the present problem.

Even though the model that we use seems more appropriate for an impurity in a solid, it is expected to be useful also for simulations on VR in liquids. Our contention that the existence of a sharp cutoff in the frequency spectrum is its most important characteristic as far as VR is concerned implies that VR in liquids should not be much different than in solids. The similarity of N_2 behavior in both phases[1,3,4] might be an indication for the validity of this viewpoint.

The results presented in this work are based on a one-dimensional geometry where the three-dimensional nature of the solid is taken into account only in the form chosen for its mode density. This is of course not a restriction on the method, and three-dimensional calculations can be done. Such calculations, which we defer to future work, could yield new information on the role of rotational and librational motion in vibrational relaxation. Recent experimental work[9,10,43] suggests that such rotational motion indeed plays an essential role in the VR process.

[1]D. S. Tinti and G. W. Robinson, J. Chem. Phys. **49**, 3229 (1968).
[2](a) L. Abouaf-Marguin, H. Dubost, and F. Leyay, Chem. Phys. Lett. **22**, 603 (1973); (b) H. Dubost and R. Charneau, Chem. Phys. **12**, 407 (1976).
[3](a) K. Dressler, O. Oehler, and D. A. Smith, Phys. Rev. Lett. **34**, 1364 (1975); (b) W. W. Duley, O. Oehler, and D. A. Smith, Chem. Phys. Lett. **31**, 115 (1975).
[4]W. F. Calaway and G. E. Ewing, Chem. Phys. Lett. **30**, 485 (1975); J. Chem. Phys. **63**, 2842 (1975).
[5](a) V. E. Bondybey, J. Chem. Phys. **66**, 995 (1977); (b) V. E. Bondybey and A. Nitzan, Phys. Rev. Lett. **38**, 889 (1977).
[6]J. Goodman and L. E. Brus, J. Chem. Phys. **65**, 1156 (1976).
[7]V. E. Bondybey and L. E. Brus, J. Chem. Phys. **63**, 2223 (1975).
[8]A. Laubereau, D. von der Linde, and W. Kaiser, Phys. Rev. Lett. **28**, 1162 (1972); A. Laubereau, G. Kehl, and W. Kaiser, Opt. Commun. **11**, 74 (1974); A. Laubereau, L. Kirscher and W. Kaiser, Opt. Commun. **9**, 182 (1973).
[9]V. E. Bondybey and L. E. Brus, J. Chem. Phys. **63**, 794

(1975).
[10]L. E. Brus and V. E. Bondybey, J. Chem. Phys. **63**, 786 (1975).
[11]J. Goodman and L. E. Brus, J. Chem. Phys. **65**, 3146 (1976).
[12]A. Nitzan and J. Jortner, Mol. Phys. **25**, 713 (1973).
[13]A. Nitzan, S. Mukamel, and J. Jortner, J. Chem. Phys. **60**, 3929 (1974); **63**, 200 (1975); J. Jortner, Mol. Phys. **32**, 379 (1976).
[14]D. J. Diestler, J. Chem. Phys. **60**, 2692 (1974).
[15]A. Nitzan and R. J. Silbey, J. Chem. Phys. **60**, 4070 (1974).
[16]S. H. Lin, J. Chem. Phys. **61**, 3810 (1974); S. H. Lin, H. P. Lin, and D. Knittel, J. Chem. Phys. **64**, 441 (1976).
[17](a) V. Yakhot, M. Berkowitz, and R. B. Gerber, Chem. Phys. **10**, 61 (1975); (b) V. Yakhot, Phys. Status Solidi B **74**, 451 (1976); (c) D. M. Derkowitz and R. B. Gerber, Chem. Phys. Lett. **49**, 260 (1977); *ibid.* (to be published).
[18]H. Y. Sun and S. A. Rice, J. Chem. Phys. **42**, 3826 (1965).
[19](a) J. J. Markham, Rev. Mod. Phys. **31**, 956 (1959); (b) Yu. E. Perlin, Sov. Phys. Vsp. **6**, 542 (1964); (c) K. K. Rebane, *Impurity Spectra of Solids* (Plenum, New York, 1970); (d) *Nato Advance Study Institute on Optical Properties of Ions in Solids*, edited by B. Di Bartolo (Plenum, New York, 1975).
[20]K. F. Freed and J. Jortner, J. Chem. Phys. **52**, 6272 (1970).
[21]S. F. Fischer and A. Laubereau, Chem. Phys. Lett. **35**, 6 (1975).
[22]D. W. Oxtoby and S. A. Rice, Chem. Phys. Lett. **42**, 1 (1976).
[23]D. J. Diestler, Chem. Phys. Lett. **39**, 39 (1976); Mol. Phys. **32**, 1091 (1976).
[24]See P. K. Davis and I. Oppenheim, J. Chem. Phys. **57**, 505 (1972), and references therein.
[25]For reviews see (a) A. Laubereau and W. Kaiser, Ann. Rev. Phys. Chem. **26**, 83 (1975); (b) M. J. French and D. A. Long, Mol. Spectrosc. Spec. Rep. **4**, 225 (1976).
[26]A. Laubereau, Chem. Phys. Lett. **27**, 600 (1974).
[27](a) H. Metiu, D. W. Oxtoby, and K. F. Freed, Phys. Rev. A **15**, 361 (1977); (b) K. F. Freed and H. Metiu, Chem. Phys. Lett. **48**, 262 (1977); (c) K. F. Freed, D. L. Yeager, and H. Metiu, Chem. Phys. Lett. **49**, 19 (1977).
[28]R. G. Gordon, J. Chem. Phys. **40**, 1973 (1964); **42**, 3658 (1965); **48**, 1302 (1965).
[29]W. G. Rothschild, J. Chem. Phys. **65**, 2958 (1976); T. Tokuhiro and W. G. Rothschild, J. Chem. Phys. **62**, 2150 (1975); A. A. Maradudin, Solid State Phys. **18**, 273 (1966).
[30]A. H. Zewail, T. E. Orlowski, R. R. Shah, and K. E. Jones, Chem. Phys. Lett. **49**, 520 (1977).
[31]E. Fermi, J. Pasta, and S. Ulam, *Collected Papers of E. Fermi, Vol. II* (University of Chicago Press, Chicago, 1965), p. 277.
[32]N. Saito, N. Ooyama, Y. Aizawa, and H. Hirooka, Prog. Theor. Phys. Suppl. **45**, 209 (1970).
[33]J. Ford, J. Math. Phys. **2**, 387 (1961); J. Ford and J. Waters, J. Math. Phys. **4**, 1293 (1963).
[34]J. Ford, Adv. Chem. Phys. **24**, 155 (1973).
[35]J. P. Riehl and D. J. Diestler, J. Chem. Phys. **64**, 2593 (1976).
[36]S. A. Adelman and J. D. Doll, J. Chem. Phys. **64**, 2375 (1976).
[37](a) S. A. Adelman and B. J. Garrison, J. Chem. Phys. **65**, 3751 (1976); (b) J. D. Doll and D. R. Dion, J. Chem. Phys. **65**, 3762 (1976).
[38]M. Shugard, J. C. Tully, and A. Nitzan, J. Chem. Phys. **66**, 2534 (1977).
[39]A. Nitzan, M. Shugard, and J. C. Tully (to be published).
[40]We have compared the results obtained using a complete Lennard-Jones potential to those obtained from a fit of its repulsive part to an exponential. For the parameters of Table I the results are almost identical.
[41]V. E. Bondybey and C. Fletcher, J. Chem. Phys. **64**, 3615 (1976); V. E. Bondybey (personal communication).
[42]Note that Tables IV and V each contain one entry for which the energy relaxation time is shorter than the dephasing time. The reader should be reminded that when all dephasing originates from energy relaxation, the dephasing time will be twice the energy relaxation time. This is a trivial outcome of the relation $E \sim \langle X^2 \rangle$.
[43]J. Wiesenfeld and C. B. Moore, Bull. Am. Phys. Soc. **21**, 1289 (1976), abstract BC13.